Transition Metal Chemistry **28**: 122–131, 2003.
© 2003 *Kluwer Academic Publishers. Printed in the Netherlands.*

Laser synthesis of transition metal clusters

J. Scott McIndoe
Department of Chemistry, The University of Cambridge, Lensfield Road, Cambridge CB2 1EW, UK

Received 12 September 2002; accepted 30 September 2002

Abstract

Laser ablation of a variety of quite different precursors has been shown to generate gas-phase clusters, which can be immediately characterised using a mass spectrometer. Such experiments provide access to a huge range of species inaccessible by more conventional preparative means. Metal oxides, phosphides and chalcogenides, metal carbonyl clusters and even giant keplerate spheres have been shown to aggregate in the gas phase to form high-nuclearity clusters.

Introduction

Laser desorption/ionisation (LDI) has achieved real popularity as a means of creating gas-phase ions only in the last 15 years, since the introduction of matrix assistance of the desorption process. In 1988, matrix-assisted laser desorption/ionisation (MALDI) was independently introduced by two groups. Tanaka *et al.* used an inorganic cobalt powder matrix [1], whereas Hillenkamp employed acidic organic molecules with a suitable UV chromophore [2]. MALDI is a 'soft' ionisation technique, due to the large excess of matrix and its high molar absorptivity coefficient resulting in the matrix absorbing most of the energy imparted by the laser. Matrices minimise gas-phase reaction and recombination of ions (and neutrals) in the laser plume, and it is exactly these processes that result in cluster formation. As such, laser cluster synthesis eliminates the use of a matrix, but investigators otherwise use the same instruments. Mass analysis is usually carried out using a time-of-flight (TOF) mass analyser, which is well suited to the pulsed ionisation technique. TOF instruments also have a very high mass range (routinely out to 100,000 m/z), a property that is very useful for the study of clusters with high molecular masses. TOF instruments have become increasingly sophisticated, with improvements in timing electronics and innovations such as delayed extraction and reflectron analysers all contributing to the high resolution now achievable [3].

Fourier transform ion cyclotron resonance (FTICR) mass spectrometers [4] are also compatible with pulsed sources, as they detect and record all masses at once, and they have proved particularly powerful in the study of clusters ablated by lasers from solid material. While lacking the mass range of TOF instruments, FTICR machines have numerous advantages, not least of which is their extraordinarily high resolution (over 100,000 for small molecules). FTICR instruments trap ions for extended periods, so gas-phase reactivity studies can be carried out [5], this topic, however, is beyond the scope of this review.

The lasers used in LDI studies are usually N_2 gas or neodymium–yttrium garnet (Nd–YAG), which emit at 337 and 1064 nm, respectively (the latter is often frequency doubled to 532 nm or quadrupled to 266 nm). Power densities are usually about 10^7–10^8 W cm^{-2}, and multiple laser pulses are averaged to improve signal-to-noise ratio [6]. Cluster synthesis is often described as being carried out by laser ablation (LA) or direct laser vapourisation (DLV), but both represent essentially the same process as LDI. LA is a more general term and encompasses any technique in which lasers are used to remove material from a surface [7]; DLV seems to have lost currency. For the purposes of this review, LDI, LA and DLV will be regarded as synonymous.

Because the laser delivers a pulse of energy in a very short time period (a few ns), the sample increases in temperature very rapidly to several thousand degrees, resulting in a laser plume containing energetic ions, neutrals and electrons. Gas-phase reactions and cluster formation occur in this hot cloud of particles, before the ions are drawn into the mass spectrometer.

This review will not deal with more elaborate two-stage gas-phase syntheses of clusters, such as where a metal is ablated directly into a reactive gas [8], or where gas-phase reactions are used to form new species from laser-generated clusters; the gas-phase coordination chemistry of transition metal ions, including clusters, has been recently reviewed [9].

Metal oxides

Early experiments using lasers to generate clusters include those carried out by Wilkins, who used noble metal oxides (Ag_2O, Au_2O_3) to generate gold and silver

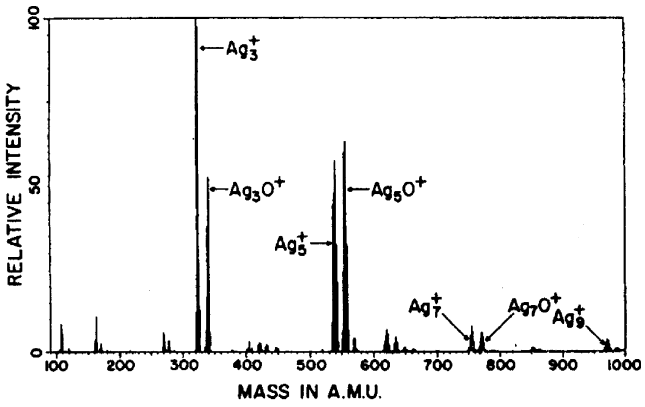

Fig. 1. Mass spectrum of Ag_n^+ ($n = 1$–9) generated by direct laser desorption from a mixed AgO/ZnO pellet. Reproduced from Ref. [12] by permission of the American Institute of Physics.

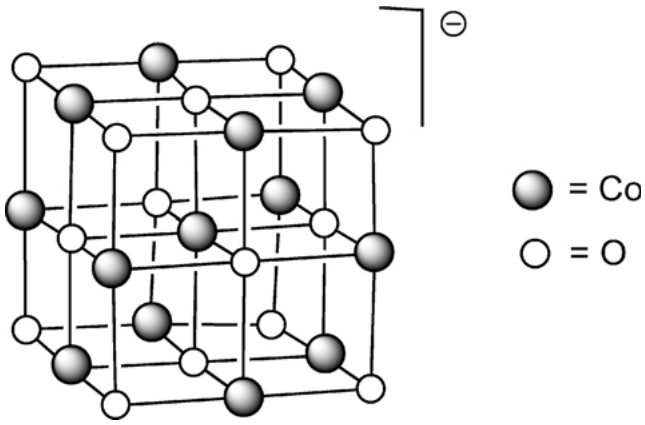

Fig. 2. Possible structure of the $[Co_{13}O_{14}]^-$ cluster anion.

dimer and trimer cations and gold dimer and trimer anions [10]. Freiser, an LDI–FTMS pioneer [11], similarly found that laser desorption of AgO and ZnO produced bare metal cluster ions [12]. Desorption from a mixture of AgO and ZnO enhanced the silver clusters at the expense of the zinc. Figure 1 shows the low level of oxygenation of the clusters and the relatively low nuclearities observed.

In contrast, direct LDI performed on a pellet of copper oxide generated an extensive series of positive and negative cluster ions $[Cu_nO_m]^{\pm}$ (positive ions: $n = 1$–14, $m = 0$–8; negative ions: $n = 1$–21, $m = 0$–12) [13]. Other groups have since studied other transition metal oxides. Cassady *et al.* characterised the clusters generated by laser desorption of MoO_2 and usefully compared the results using two different lasers, pulsed CO_2 and Nd:YAG [14]. The spectra were largely similar, but with extra species of the type $(MoO_3)_n^+$ generated with the CO_2 laser. This difference was attributed to the fact that molybdenum oxides absorb strongly at the CO_2 wavelength of 10.6 μm, but not at the Nd:YAG wavelength of 532 nm. Muller *et al.* [15] have made more recent studies on TiO_2, alone and mixed with lead oxides. The titanium clusters could largely be described by series derived from sequential addition of neutral TiO_2 to the precursor ions Ti^+, TiO^+ and TiO_2^+. Huge titanium oxide aggregates (up to 50 metal atoms) from TiO_2 were reported elsewhere in the same year [16]. Muller's group also studied 19 different chromium oxide species, and found a similar aggregative effect, this time between $[CrO_2]^-$ or $[CrO_3]^-$ ions and CrO_2 and/or CrO_3 neutrals [17]. They also found MO_3 (M = Cr, Mo, W) to generate highly oxygenated cluster ions under laser desorption conditions, in contrast to other transition metal oxides [18]. A study on oxides of first-row transition metals (Mn, Fe, Co, Ni, Cu), confirmed that negatively charged cluster anions $[M_xO_y]^-$ are generated, and it was found that stoichiometrically different oxides gave similar collections of anions [19]. A recent, detailed study of the laser desorption of Co_3O_4 by Dance *et al.* showed that 26 gaseous binary anions of the type $[Co_xO_y]^-$ ($x = 1$–13, $y = 2$–14) were formed [20]. The most interesting of these was perhaps the largest, $[Co_{13}O_{14}]^-$, which may have a structure similar to the unit cell of NaCl (Figure 2, Table 1).

Metal phosphides and chalcogenides

The group of Dance and Fisher have been primarily responsible for the introduction of gas-phase cluster chemistry to the mainstream inorganic chemistry community. Previously, this area was the domain of physical chemists and mass spectrometrists. Interest in these 'exposed molecules' exists partly because of their position between the extremes of non-molecular solids and ligated, molecular clusters [21].

Many of the first-row transition metal chalcogenides have been studied by this group. A study [22], on the nickel sulphides NiS and Ni_3S_2 showed that the set of $[Ni_xS_y]^-$ ions formed was largely independent of the chemical composition of the sample ablated, indicating that it is unlikely that the clusters are excised intact from the solid, but rather they are formed in the laser plume. An earlier study, using an isotopically labelled sample of ^{34}S + NiS, also found that gas-phase recombination occurred [23]. Studies on CuS, Cu_2S and KCu_4S_3 confirmed this pattern, and it was also shown that mixtures of Cu and E (E = Se, Te) gave very similar ion distributions under LA as Cu_2E [24]. Silver [25], cobalt and iron [26] sulphides all produced extensive series of negatively charged cluster ions of the type $[M_xS_y]^-$, and no less than 83 stoichiometrically unique anionic clusters were generated by LA of CoS. The studies have also generally shown that few cationic clusters are formed, suggesting that their generation is *via* a different path to that of the anionic clusters. It seems likely that ablation probably does not form negative ions directly, but the presence of neutral clusters with high electron affinity and free electrons in the plume could account for the large population of negative ions observed.

Table 1. LA of metal oxides

Ablated material	Largest binary cluster observed	Number of ions observed[a]	Comments	Ref.
Au_2O_3	$[Au_3]^-$	3−	No oxide clusters	[10]
	$[Au_3]^+$	3+		
AgO + ZnO	$[Ag_9]^+$	7+	Some Ag_nO^+ species, no Zn containing clusters	[12]
CuO	$[Cu_{21}O_{12}]^-$	20−		[13]
	$[Cu_{14}O_8]^+$	15+		
MoO_2	$[Mo_4O_{12}]^-$	7−	Pulsed CO_2 and Nd:YAG lasers compared; results were similar	[14]
	$[Mo_4O_{11}]^+$	15+		
TiO_2	$[TiO_3(TiO_2)_n]^-$	10−	n = 1–3	[15]
	$[TiO(TiO_2)_n]^+$	10+		
PbO/TiO_2, $Pb_3O_4/3TiO_2$, $PbTiO_3$	$[TiO_2(TiO_2)_n]^-$	25−	n = 1–17, m = 1–4. Mixed-metal species a minor component only	[15]
	$[PbO(PbO)_m]^+$	15+		
TiO_2	$[TiO(TiO_2)_{n-1}]^+$	100+	n = 1–50	[16]
	$[(TiO_2)_n]^+$			
$Cr_2(SO_4)_3 \cdot xH_2O$	$[Cr_5O_{11}]^-$	13−	18 other chromium compounds studied	[17]
	$[Cr_8O_{16}]^+$	21+		
CrO_3	$[Cr_4O_{11}]^-$	9−	Highly oxygenated clusters	[18]
	$[Cr_6O_{13}]^+$	18+		
MoO_3	$[Mo_6O_{17}]^-$	20−	Highly oxygenated clusters	[18]
	$[Mo_6O_{18}]^+$	7+		
WO_3	$[W_4O_{12}]^-$	4−	Highly oxygenated clusters	[18]
	$[W_4O_{12}]^+$	15+		
Co_3O_4	$[Co_{13}O_{14}]^-$	26−	$[Co_{13}O_{14}]^-$ may have structure of the NaCl unit cell	[20]

[a] These numbers are either mentioned by the authors or are conservative estimates based on the published data.

The advantage of high mass resolution is revealed if contemporaneous spectra from the LA of $KFeS_2$ studied by FTMS [26] and that of Fe + S studied by TOF [27] are compared (Figure 3).

TOF instruments are now capable of much higher resolution (though still less than FTMS instruments), and are better able to provide unambiguous assignments. The lower pressures that TOF instruments operate under means that metal/sulphur mixtures can be readily studied, as such experiments are limited with FTMS due to the relatively high vapour pressure of S_8. The group of Gao has taken advantage of this and conducted studies on Fe + S and Ta + S [28], and other investigations on related systems such as Cr + P [29]. Their studies of Ag + Se, Cr + S, Ag + S, Ag + Se, Fe + P and Mn + Se have been reported in the Chinese literature[1]. These reports generally seem to show that the suites of clusters generated by LA of mixtures are similar to those prepared from the metal chalcogenides. Manganese sulfide appears to be one example in which the source of metal and chalcogenide is important. LA of metastable pink MnS gave significantly different ion abundances to the green form [30].

Metal phosphides have also been subjected to LA, and some spectacularly extensive sets of clusters have been produced. Most notable is the 152 binary anionic cobalt phosphide clusters $[Co_xP_y]^-$ generated from CoP, with the largest cluster $[Co_{25}P_{16}]^-$ [31]. Similarities exist between the spectra obtained from CoP and that from Co + P [32]. The main difference between the two is that the $[Co_xP_y]^-$ ions from CoP tend to be P-deficient, while the ions from Co + P are P-rich, the explanation for which is based on the higher volatility of red phosphorus compared to cobalt metal. CoP necessarily produces a 1:1 ratio of Co:P in the plume. Density functional calculations were carried out on a number of different species observed in the mass spectrum. Examples of the isomers optimised for $[Co_4P_8]^-$ are shown in Figure 4; it was concluded that isomer 48C was the most probable (Table 2).

Other non-molecular precursors

Solid MCN (M = Cu, Ag) produced a relatively low mass series of clusters with the general formula $[M_n(CN)_{n+1}]^-$ (M = Cu, n = 1–5; M = Ag, n = 1–4) and $[M_n(CN)_{n+1}]^+$ (M = Cu, n = 1–6; M = Ag, n = 1–4). A mixture of CuCN and AgCN produced some mixed metal clusters. Calculations show that the most likely geometries for these clusters are linear alternations of M and CN [33]. LA of a mixture of cobalt and germanium generated a series of binary clusters $[Co_xGe_y]^-$, with a notably high abundance for the $[CoGe_{10}]^-$ cluster [34].

Gold cluster ions, $Au_n^{\pm}$ (n = 1–46) can be generated directly from laser desorption of peptide-covered thin gold films [35]. Using a particularly high powered

[1] Abstracts from ISI Web of Science.

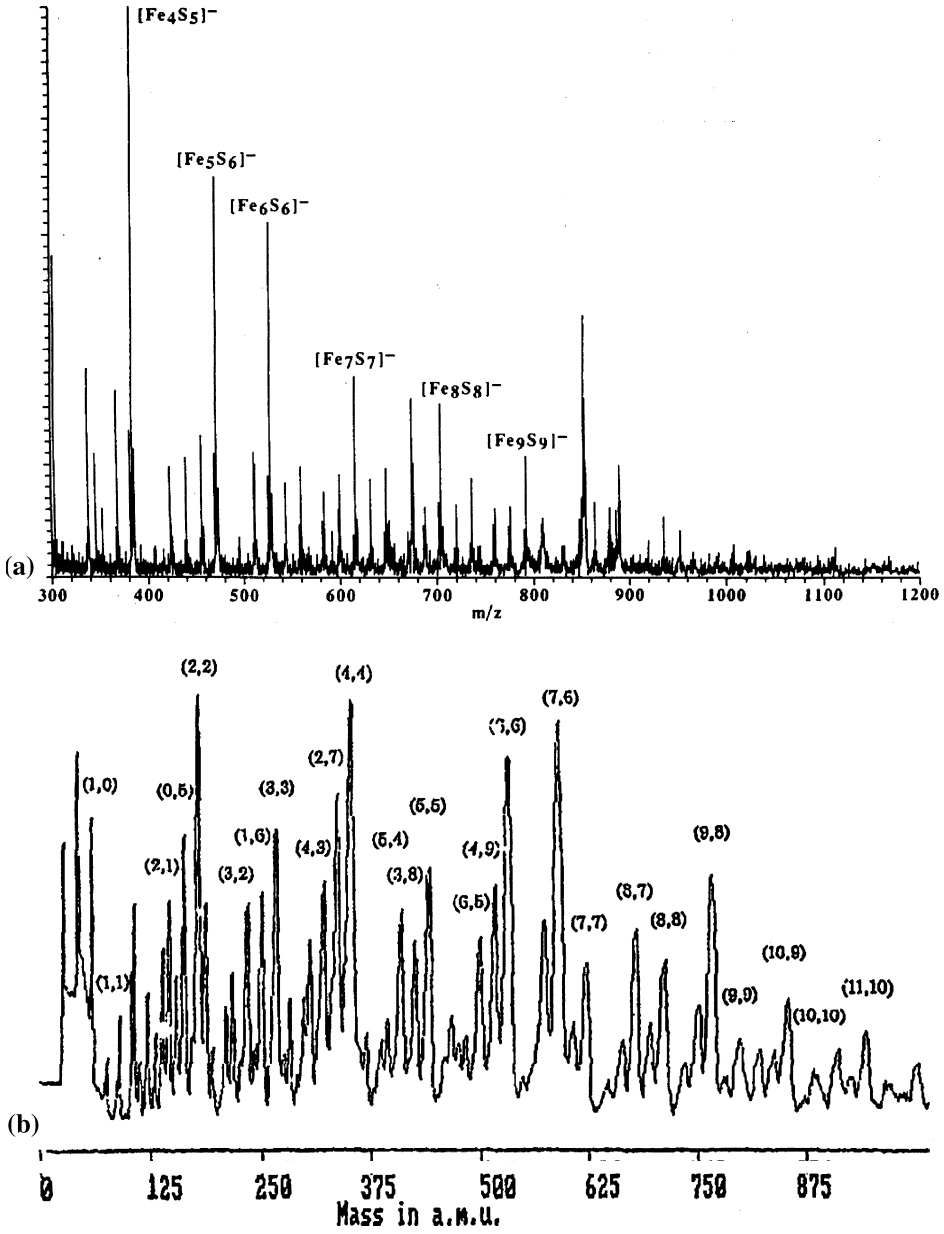

Fig. 3. (a) Negative-ion FTICR mass spectrum of laser-ablated $KFeS_2$. Reprinted with permission from Ref. [26]. Copyright 1993 American Chemical Society. (b) Positive-ion TOF mass spectrum of $[Fe_xS_y]^+$ cluster ions. Reproduced from Ref. [27] by permission of the American Institute of Physics.

nitrogen laser, extremely large gold clusters have been synthesised from a metallic gold target, including doubly charged anions (Figure 5) [36]. The size of the cluster formed increased with the laser fluence.

Large, positively and negatively charged silver clusters containing up to 100 silver atoms have been generated in the gas phase by the LDI of silver-containing salts [37]. The cluster distributions were observed to resemble those generated by molecular beam methods.

Transition metal carbonyl cluster precursors

Mass spectrometry of high-nuclearity metal carbonyl clusters using the traditional technique of electron impact (EI) ionisation is not trivial, due to the thermal fragility and very low volatility of such compounds. Clusters with molecular weights much in excess of 1000 m/z are in practice inaccessible to EI. Fast atom bombardment (FAB) relies on chemical ionisation by a liquid matrix, typically protonation, and the very low basicity of carbonyl clusters means that this technique is often unreliable [38]. The new technique of MALDI–TOFMS appeared to offer a simple means of obtaining molecular weight information on high-nuclearity clusters. However, the first investigations revealed that something much more complicated than simple ionisation and/or fragmentation was occurring [39]. A series of high mass peaks appeared in the spectrum, representing large aggregates of ligated metal atoms in multiples

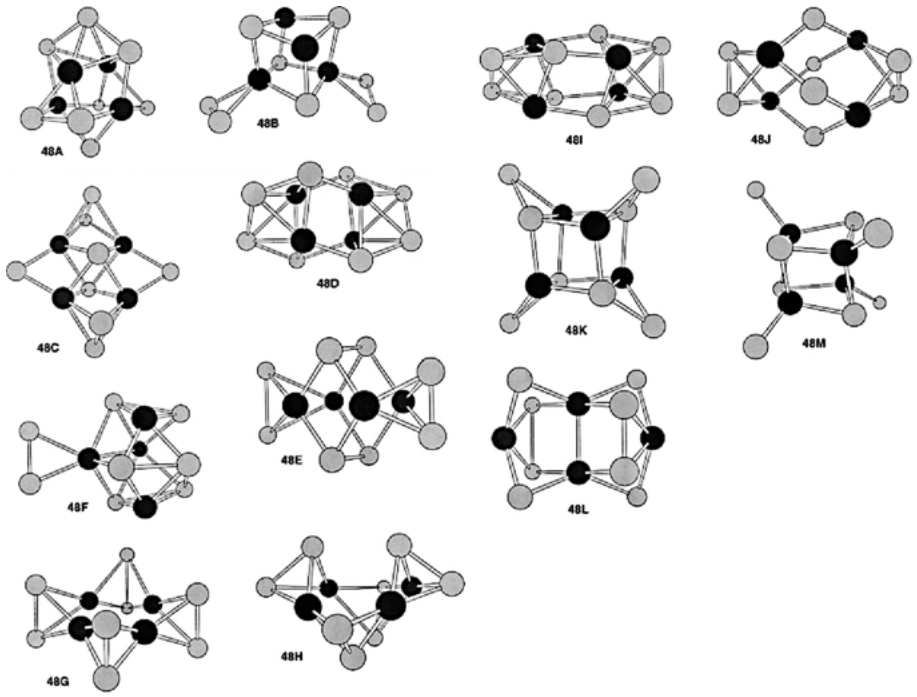

Fig. 4. The structures of isomers of $[Co_4P_8]^-$, as optimised by density functional calculations. Black is Co, grey is P. Reprinted with permission of The Royal Society of Chemistry from Ref. [32].

Table 2. LA of metal chalcogenides and phosphides

Ablated material	Largest binary cluster observed	Number of ions observed*	Comments	Ref.
Ni_3S_2 or NiS	$[Ni_{15}S_{10}]^-$	28–	Ni + S limited by vapour pressure of S_8	[22]
CuS, Cu_2S, KCu_4S_3	$[Cu_{21}S_{11}]^-$	23–	Many larger species observed, but not unambiguously	[24]
Cu_2Se or Cu + Se	$[Cu_{17}Se_9]^-$	20–		[24]
Cu_2Te or Cu + Te	$[Cu_{19}Te_{10}]^-$	17–		[24]
Ag_2E (E = S, Se, Te)	$[Ag_{21}E_{11}]^-$	> 20–		[25]
CoS	$[Co_{38}S_{24}]^-$	83–		[26]
$KFeS_2$ or FeS	$[Fe_{11}S_{10}]^-$	45–		[26]
Fe + S	$[Fe_{13}S_{13}]^+$	> 30 +		[27]
Ta + S	$[Ta_9S_{30}]^+$	> 30 +		[28]
Cr + P	$[Cr_8P_{14}]^+$	> 20 +		[29]
MnS	$[Mn_{22}S_{23}]^-$	66–	$[Mn_xS_xO]^-$ ions also observed; differences between polymorphs	[30]
CoP	$[Co_{25}P_{16}]^-$	152–		[31]
Co + P	$[Co_{12}P_{16}]^-$	110–		[32]
Ni + P	$[Ni_{10}P_{11}]^-$	37–		[32]

Table 3. LA of miscellaneous non-molecular precursors

Ablated material	Largest binary cluster observed	Number of ions observed*	Comments	Ref.
CuCN	$[Cu_5(CN)_6]^-$	5–	Linear clusters	[33]
	$[Cu_6(CN)_5]^+$	6+		
AgCN	$[Ag_4(CN)_5]^-$	5–	Linear clusters	[33]
	$[Ag_4(CN)_3]^+$	7+		
Equimolar CuCN/AgCN	$[Ag_2Cu_2(CN)_6]^-$	5–	Linear clusters	[33]
	$[Ag_2Cu_3(CN)_4]^+$	8+		
Co + Ge	$[Co_6Ge_{20}]^-$	20–	$[CoGe_{10}]^-$ especially intense.	[34]
Au	$[Au_{100}]^-$, $[Au_{200}]^{2-}$	300–	Anions and dianions	[36]
	$[Au_{90}]^+$	90+		
Pt	$[Pt_{60}]^-$	60–		[36]
	$[Pt_3]^+$	3+		

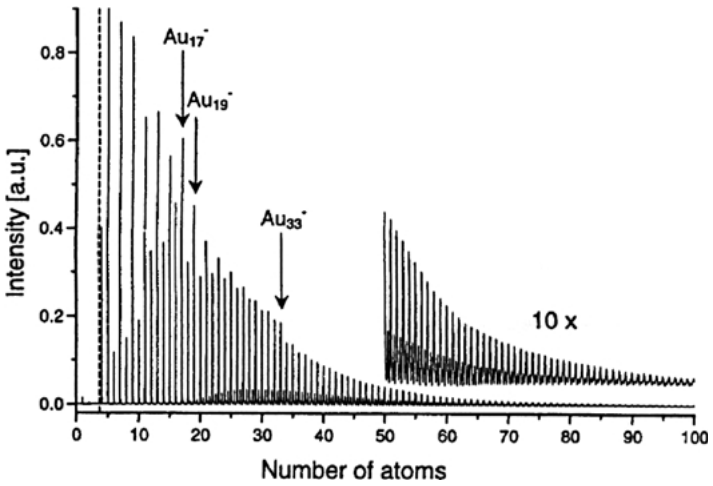

Fig. 5. Mass spectrum of clusters formed upon pulsed N_2 LA of a polycrystalline gold target: negative ions at 5 μs after ablation. Reproduced with the permission of Elsevier Science from Ref. [37].

of the original nuclearity of the cluster. This phenomenon is illustrated in Figure 6 for the hexaruthenium cluster $Ru_6C(CO)_{17}$. An extensive series of high mass signals were observed in the negative-ion mode that could be attributed to $[Ru_6C(CO)_n]_m$, where m ranged from one to at least 25.

Very similar results were obtained for the substituted hexaruthenium carbide clusters $Ru_6C(CO)_{14}(\eta^6\text{-}C_6H_5\text{-}Me)$ and $Ru_6C(CO)_{12}(\eta^6\text{-}C_6H_5Me)(\eta\text{-}C_6H_7Me)$. Aggregates in multiples of six ruthenium atoms appeared in the spectra, but with some evidence for suppression of the supraclustering process by the arene ligands. The positive-ion mode produced similar spectra, but with significantly lower ion currents. No useful molecular weight information was generated for any of the clusters, and molecular ions were absent in the negative-ion spectra in all cases. This observation can be explained by the fact that in the plume, the electronically saturated neutral cluster will not be susceptible to electron attachment, whereas those species that have lost CO ligands will have significant electron affinities. However, electronically saturated clusters are just as susceptible to electron loss, explaining the presence of $[M]^+$ molecular ions.

Further studies were carried out on $M_3(CO)_{12}$ (M = Fe, Ru, Os) [40], which showed significantly different behaviour. Instead of cluster aggregation occurring without fragmentation, the trinuclear clusters appear to break apart, then recombine in the plume to form higher nuclearity clusters. The extent to which this occurs is lower than for the hexanuclear clusters, with the trinuclear clusters forming supraclusters of nuclearity of 1 to >50 for $Fe_3(CO)_{12}$, 2–9 for $Ru_3(CO)_{12}$ and 3–11 for $Os_3(CO)_{12}$. Supraclustering occurs in both positive- and negative-ion modes. Figure 7 shows the negative-ion LDI–TOF mass spectrum of $Ru_3(CO)_{12}$.

Notable are the presence of species as yet inaccessible to conventional synthetic techniques, such as $[Ru_4(CO)_{13}]^-$, $[Ru_5(CO)_{15}]^-$, $[Ru_6(CO)_{18}]^-$, $[Ru_7(CO)_{20}]^-$, $[Ru_8(CO)_{22}]^-$ and $[Ru_9(CO)_{24}]^-$, which correspond to

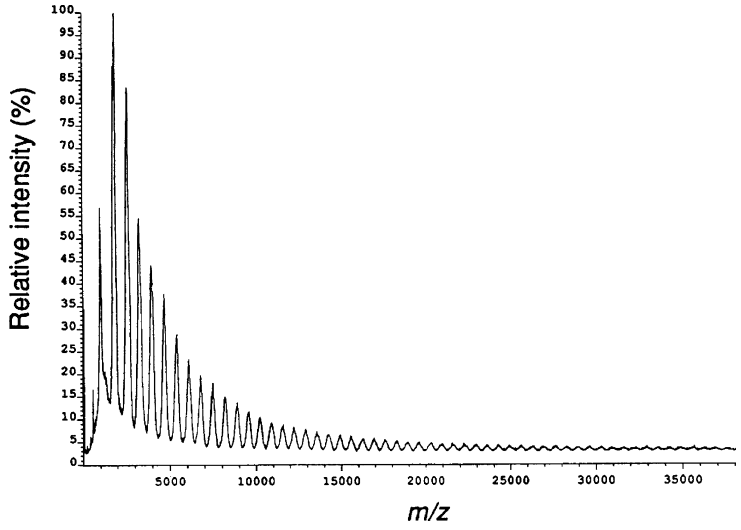

Fig. 6. The negative-ion LDI–TOF mass spectrum of $Ru_6C(CO)_{17}$. Reprinted with permission of The Royal Society of Chemistry from Ref. [40].

the neutral ruthenium clusters $Ru_4(CO)_{14}$, $Ru_5(CO)_{16}$, $Ru_6(CO)_{19}$, $Ru_7(CO)_{21}$, $Ru_8(CO)_{23}$ and $Ru_9(CO)_{25}$. All of these clusters have well-characterised osmium analogues, but all are unknown, doubtless due to the lack of suitable synthetic routes (the ruthenium carbide cluster $Ru_6C(CO)_{17}$ is a thermodynamic sink in high-nuclearity ruthenium carbonyl chemistry) [41]. Laser synthesis would seem to be one approach to accessing these clusters, though scaling up the preparation would no doubt involve experimental difficulties.

An independent study of $M_3(CO)_{12}$ (M = Fe, Ru, Os) by LA claimed that fragmentation occurred not only by CO loss but also by expulsion of O_2; however, this conclusion seems unjustifiable in light of the quality of the data [42] (Table 4).

Investigation of the phosphine substituted ruthenium clusters $Ru_3(CO)_{12-n}(PPh_3)_n$ ($n = 1$, 2, 3) gave similar results as $Ru_3(CO)_{12}$, with the complete absence of PPh_3 ligands in any of the spectra and more extensive fragmentation [43]. The acetonitrile-substituted osmium cluster, $Os_3(CO)_{10}(NCMe)_2$, also underwent increased fragmentation and aggregation processes, and the NCMe ligands did not appear in the spectrum, [44]. Both PPh_3 and NCMe are poorer ligands than CO, so are preferentially lost in the high-temperature ablation process. The hexanuclear clusters $Rh_6(CO)_{16}$ and $Os_6(CO)_{18}$ have also been studied by LDI–TOFMS; both underwent extensive supraclustering processes reminiscent of the hexaruthenium clusters [45].

The trinuclear hydrido clusters $H_3M_3(CO)_{12}$ (M = Mn, Re) supracluster under LDI conditions to produce series of clusters of the general formula $[H_{n-1}M_n(CO)_{4n}]^-$ (where $n = 3$–9 for Mn and 3–6 for Re) [46]. The negative-ion spectrum for $H_3Mn(CO)_{12}$ is shown in Figures 8 and 9 shows the proposed structures of the supraclusters.

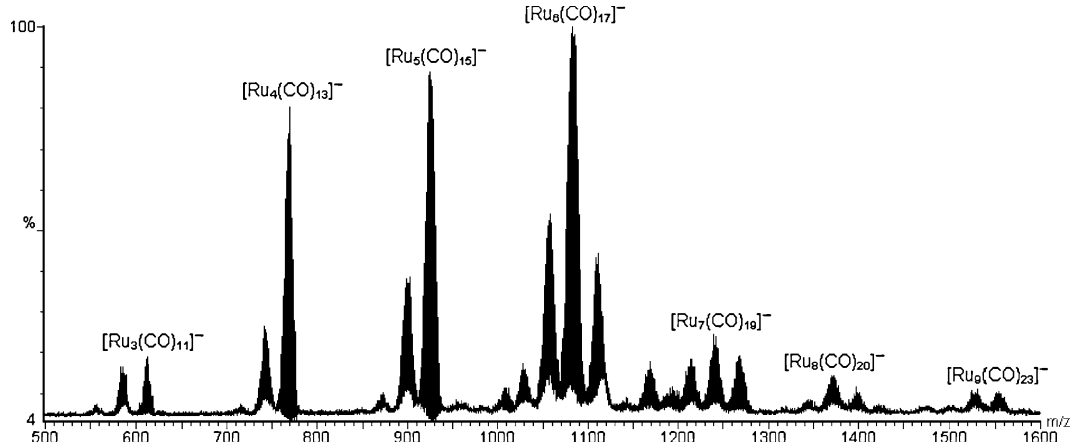

Fig. 7. Negative-ion UV laser desorption mass spectrum of $Ru_3(CO)_{12}$. Reprinted with permission from Ref. [41]. Copyright 1998 American Chemical Society.

Table 4. LA of carbonyl cluster precursors

Ablated cluster	Largest cluster observed	Multiples of original nuclearity observed	Comments	Ref.
$Ru_6C(CO)_{17}$	$[(Ru_6C)_{30}(CO)_x]^+$	1–30+		[39]
$Ru_6C(CO)_{14}(\eta^6\text{-}C_6H_5Me)$	$[(Ru_6C_8H_8)_{12}(CO)_x]^+$	1–12	Arene ligands not lost	[39]
$Ru_6C(CO)_{12}(\eta^6\text{-}C_6H_5Me)$-$(\eta\text{-}C_6H_7Me)$	$[(Ru_6C_{15}H_{18})_{20}(CO)_x]^+$	1–20	Arene ligands not lost	[39]
$Fe_3(CO)_{12}$	$[Fe_{12}(CO)_{24}]^-$	Core fragmentation and aggregation observed	Ambiguity in peak assignments due to the similarity in mass between [Fe] and [2CO]	[40]
$Ru_3(CO)_{12}$	$[Ru_9(CO)_{23}]^-$	Core fragmentation and aggregation observed		[40]
$Os_3(CO)_{12}$	$[Os_8(CO)_{22}]^-$	Core fragmentation and aggregation observed		[40]
$Ru_3(CO)_{12-n}(PPh_3)_n$ ($n = 1$, 2, 3)	$[Ru_9(CO)_{23}]^-$	Core fragmentation and aggregation observed	Overall similarity to $Ru_3(CO)_{12}$; no phosphine ligands in supraclusters	[43]
$Os_3(CO)_{10}(NCMe)_2$	$[Os_8(CO)_{22}]^-$	Core fragmentation and aggregation observed		[44]
$Os_6(CO)_{18}$	$[Os_{30}(CO)_x]^-$	1–5		
	$[Os_{30}(CO)_x]^+$	1–5		[44]
$Rh_6(CO)_{16}$	$[Rh_{60}(CO)_x]^-$	1–10	Extensive PSD	[45]
$H_3M_3(CO)_{12}$ (M = Mn, Re)	$[H_8Mn_9(CO)_{36}]^-$	1–10	Formation of large cyclic species	[46]

It seems likely that the key step in formation of these cyclic species is formation of the highly reactive fragment $[MH(CO)_4]$, with aggregation and proton loss occurring in the plume to give the observed species.

Further investigations into a range of other clusters have provided more insight into the supraclustering process; however, it has proved difficult to tune the desorption process in such a way as to maximise the yield of a given product (P. J. Dyson *et al.* unpublished data).

Other molecular precursors

Giant metal oxide spheres have been studied using MALDI, and in addition to providing molecular weight information on the keplerate compounds $[Mo_{78}Fe_{30}O_{274}(H_2O)_{94}\ (CH_3COO)_{12}]\cdot\sim150H_2O$ and $[Mo_{102}O_{252}(H_2O)_{78}(CH_3COO)_{12}]\cdot\sim150H_2O$, aggregates of 2, 3, 4 and 5 such giant balls were also observed in the gas phase [47]. Figure 10 shows a representation of the giant ball structure (as characterised crystallographically) and the mass spectra of the monomers and oligomeric species.

In this case, careful selection of a suitable matrix was crucial to providing good data, which may well suggest that the mechanism of aggregation is different from the cases described above for straight LDI experiments. The authors speculate that the gas-phase assemblies may be held together either by matrix molecules or perhaps through crosslinking by covalent—M—O—M— bridges.

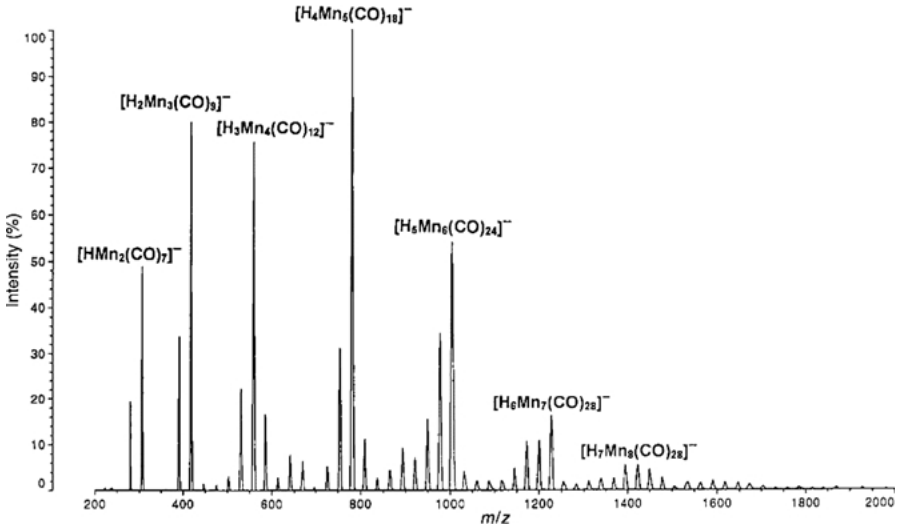

Fig. 8. Negative-ion UV LDI mass spectrum of $H_3Mn_3(CO)_{12}$. Reprinted with permission of The Royal Society of Chemistry from Ref. [47].

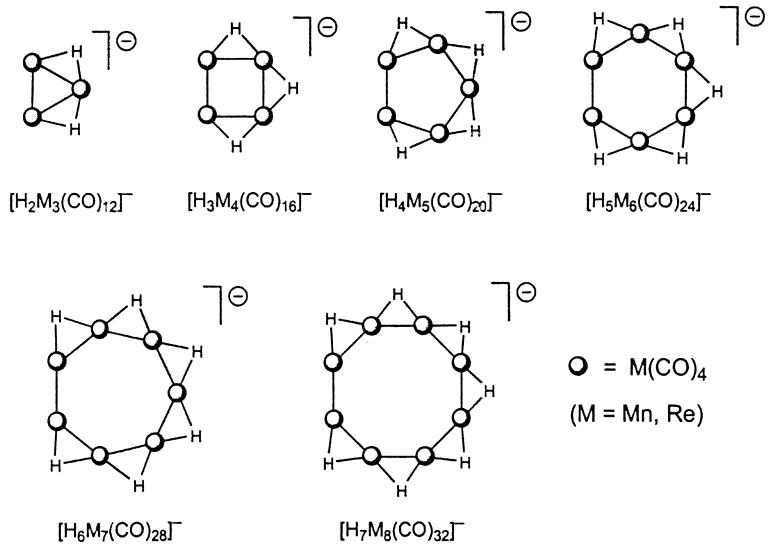

Fig. 9. Proposed structures for the species $[H_{n-1}Mn_n(CO)_{4n}]^-$ ($n = 3$–8). Reprinted with permission of The Royal Society of Chemistry from Ref. [47].

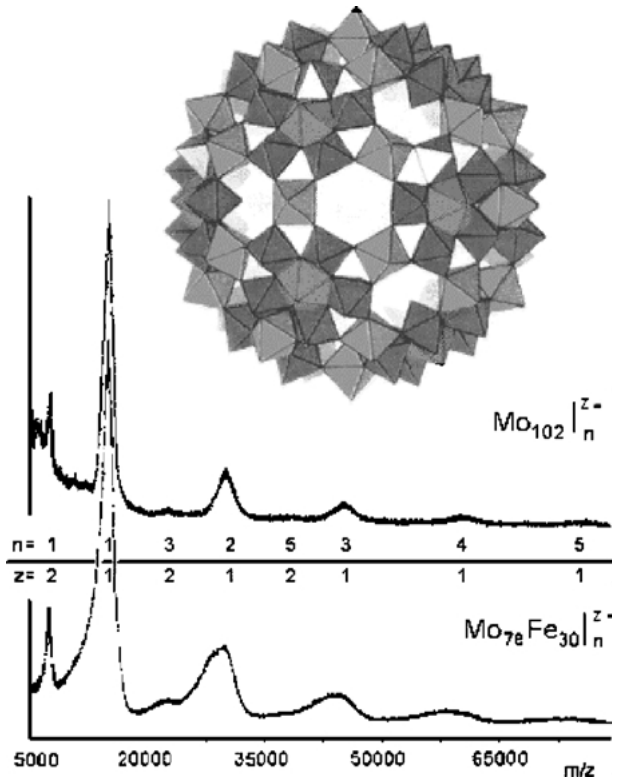

Fig. 10. Polyhedral representation of the shell of the $Mo_{72}Fe_{30}$ type keplerate (top) and MALDI–TOF mass spectra of the $Mo_{72}(Mo_6)Fe_{30}$ and Mo_{102} species and their oligomers (bottom). Reprinted with permission of The Royal Society of Chemistry from Ref. [49].

Laser desorption for cluster characterisation

In specific cases, LDI has proved reasonably effective as a characterisation tool for metal clusters [48]. Anionic transition metal carbonyl clusters provide good LDI mass spectra, with no aggregation processes apparent whatsoever, and fragmentation occurring only as simple loss of CO ligands [49]. However, some charge information is lost in the desorption process due to electron detachment, and dianionic clusters such as $[Os_{10}C(CO)_{24}]^{2-}$ give singly charged molecular ions only [50]. As such, it seems unlikely that LDI will supplant ESI as the method of choice for the characterisation of metal carbonyl clusters [51].

Laser desorption of a variety of aurothiol (Au:SR) cluster compounds results in a broad, intense peak near 29 kDa, indicating clusters of average composition $Au_{144–146}(SR)_{50–60}$ [52]. However, in this case, X-ray powder diffraction and a variety of other techniques indicate that this cluster exists intact in the solid state, and gas-phase aggregation does not seem to occur.

The phosphorus containing clusters $Fe_4(\eta^5\text{-}C_5H_4Me)_4(CO)_6P_8$ and $Fe_6(\eta^5\text{-}C_5H_4Me)_4(CO)_{13}P_8$ have been successfully characterised by LDI-FTICR mass spectrometry [53]. A comparative analysis of LDI–FTICR and EI–FTICR mass spectra of four organometallic complexes of varying volatilities, including the dimers $Fe_2(\eta\text{-}C_5Me_5)_2(\mu\text{-}P_2)_2$ and $Co_2(\eta\text{-}C_5Me_5)_2(\mu\text{-}P_2)_2$, concluded that LDI gave either similar or much superior information to that provided (if at all) by EI, especially when the target complex was thermally unstable [54]. The halide clusters $[(Nb_6X_{12})X_2(H_2O)_4]\cdot 4H_2O$ (X = Cl, Br) were studied using LDI–FTICR mass spectrometry [55]. The quasi-molecular ion $[(Nb_6X_{12})X_2]^-$ and fragment ions involving losses of 1–3 X were the most abundant in the spectrum, indicating the stability of the core cluster, Nb_6X_{12}.

The clusters $Cs_3Re_3X_{12}$ (X = Cl, Br) and $(NBu_4)_2[Re_2Cl_8]$ were examined using LDI with and without the use of a matrix [56]. MALDI produced the best spectra, and characteristic fragments due to loss of X gave peaks that were used to identify the number of rhenium atoms and the identity of the ligands, by the isotope patterns and m/z values. The same authors have since successfully extended the utility of the technique to the cluster anions $[Re_3(\mu_3\text{-}E)(\mu\text{-}Cl)_3Cl_6]^{2-}$ (E = S, Se, Te) [57]. MALDI has also been used to characterise a number of different dendritic carbosilanes containing ethynyl groups and dicobalt hexacarbonyl clusters on the periphery [58]. Molecular masses of up to 8500 Da have been successfully established [59].

Conclusions

LA of a variety of inorganic compounds results in gas-phase aggregation in the laser plume. A huge variety of novel clusters can be synthesised in this way, and immediately characterised using a suitable mass spectrometer. Theoretical techniques offer perhaps the most straightforward way of providing insight into the structures of these new species, though this is an approach which becomes more uncertain with increasingly large clusters.

Perhaps the most striking aspect of this area of research is its potential. Whole classes of compounds are waiting to be investigated by LDI–MS, and there is absolutely no reason to expect that the results will not be as rich and as varied as those already reported.

Acknowledgements

The author thanks Newnham and Trinity Colleges, Cambridge for a college lectureship.

References

1. K. Tanaka, H. Waki, Y. Ido, S. Akita, Y. Yoshida and T. Yoshida, *Rapid. Commun. Mass Spectrom.*, **2**, 151 (1988).
2. M. Karas and F. Hillenkamp, *Anal. Chem.*, **60**, 2299 (1988).
3. S.A. McLuckey and J.M. Wells, *Chem. Rev.*, **101**, 571 (2001).
4. A.G. Marshall, C.L. Hendrickson and G.S. Jackson, *Mass Spectrom. Rev.*, **17**, 1 (1998).
5. For example see I.G. Dance, K.J. Fisher and G.D. Willett, *Inorg. Chem.*, **35**, 4177 (1996).

6. D.C. Muddiman, R. Bakhtiar, S.A. Hofstadler and R.D. Smith, *J. Chem. Educ.*, **74**, 1288 (1997).
7. D.M. Lubman (Ed.) *Lasers and Mass Spectrometry*, Oxford University Press, New York (1990).
8. For examples, see: M. Foltin, G.J. Stueber and E.R. Bernstein, *J. Chem. Phys.*, **114**, 8971 (2001); R.C. Bell, K.A. Zemski, K.P. Kerns, H.T. Deng and A.W. Castleman, *J. Phys. Chem.*, **102**, 1733 (1998).
9. K.J. Fisher, *Prog. Inorg. Chem.*, **50**, 343 (2001).
10. D.A. Well and C.L. Wilkins, *J. Am. Chem. Soc.*, **107**, 7316 (1985).
11. R.C. Burnier, G.D. Byrd and B.S. Freiser, *J. Am. Chem. Soc.*, **103**, 4360 (1981).
12. S.W. Buckner, J.R. Gord and B.S. Freiser, *J. Chem. Phys.*, **88**, 3678 (1988).
13. J.R. Gord, R.J. Bemish and B.S. Frieser, *Int. J. Mass Spectrom. Ion. Proc.*, **102**, 115 (1990).
14. C.J. Cassady, D.A. Well and S.W. McElvany, *J. Chem. Phys.*, **96**, 691 (1991).
15. N. Chaoui, E. Millon and J.F. Muller, *Chem. Mater.*, **10**, 3888 (1998).
16. X.H. Liu, X.G. Zhang, Y. Li, X.Y. Wang and N.Q. Lou, *Int. J. Mass Spectrom.*, **177**, L1 (1998).
17. F. Aubriet, B. Maunit and J.F. Muller, *Int. J. Mass Spectrom.*, **209**, 5 (2001).
18. F. Aubriet and J.F. Muller, *J. Phys. Chem. A.*, **106**, 6053 (2002).
19. M.C. Oliveira, J. Marcalo, M.C. Vieira and M.A.A. Ferreira, *Int. J. Mass Spectrom. Ion. Proc.*, **187**, 825 (1999).
20. M.N. Yi, K.J. Fisher and I.G. Dance, *Int. J. Mass Spectrom.*, **216**, 155 (2002).
21. I.G. Dance, *Chem. Commun.*, 523 (1998); I.G. Dance and K.J. Fisher, *Prog. Inorg. Chem.*, **41**, 637 (1994).
22. J.H. El Nakat, I.G. Dance, K.J. Fisher, D. Rice and G.D. Willett, *J. Am. Chem. Soc.*, **113**, 5141 (1991).
23. I.H. Musselman, R.W. Linton and D.S. Simons, *Anal. Chem.*, **60**, 110 (1988).
24. J.H. El Nakat, I.G. Dance, K.J. Fisher and G.D. Willett, *Inorg. Chem.*, **30**, 2958 (1991).
25. J.H. El Nakat, I.G. Dance, K.J. Fisher and G.D. Willett, *J. Chem. Soc., Chem. Commun.*, 746 (1991).
26. J.H. El Nakat, I.G. Dance, K.J. Fisher and G.D. Willett, *Inorg. Chem.*, **32**, 1931 (1993).
27. Z.D. Yu, N. Zhang, X.J. Wu, Z. Gao, Q.H. Zhu and F.N. Kong, *J. Chem. Phys.*, **99**, 1765 (1993).
28. N. Zhang, Z.D. Yu, X.J. Wu, Z. Gao, Q.H. Zhu and F.N. Kong, *J. Chem. Soc., Faraday Trans.*, 1779 (1993).
29. C.Y. Han, X. Zhao, X. Zhang, Z. Gao and Q.H. Zhu, *Rapid Commun. Mass Spectrom.*, **14**, 1255 (2000).
30. I.G. Dance, K.J. Fisher and G.D. Willett, *J. Chem. Soc., Dalton Trans.*, 2557 (1993).
31. M. Yi, K. Fisher and I. Dance, *New J. Chem.*, **25**, 73 (2001).
32. P.F. Greenwood, I.G. Dance, K.J. Fisher and G.D. Willett, *Inorg. Chem.*, **30**, 6288 (1998).
33. I.G. Dance, P.A.W. Dean and K.J. Fisher, *Inorg. Chem.*, **33**, 6261 (1994).
34. X. Zhang, G.L. Li and Z. Gao, *Rapid Commun. Mass Spectrom.*, **15**, 1573 (2001).
35. H.S. Kim, T.D. Wood, A.G. Marshall and J.Y. Lee, *Chem. Phys. Lett.*, **224**, 589 (1994).
36. C. Stoermer, J. Friedrich and M.M. Kappes, *Int. J. Mass Spectrom.*, **206**, 63 (2001).
37. H. Rashidzadeh and B.C. Guo, *Chem. Phys. Lett.*, **310**, 466 (1999).
38. M.I. Bruce and M.J. Liddell, *Appl. Organomet. Chem.*, **1**, 191 (1987).
39. (a) M.J. Dale, P.J. Dyson, B.F.G. Johnson, P.R.R. Langridge-Smith and H.T. Yates, *J. Chem. Soc., Chem. Commun.*, 1689 (1995); (b) M.J. Dale, P.J. Dyson, B.F.G. Johnson, C.M. Martin, P.R.R. Langridge-Smith and R. Zenobi, *J. Chem. Soc., Dalton Trans.*, 771 (1996).
40. G. Critchley, P.J. Dyson, B.F.G. Johnson, J.S. McIndoe, R.K. O'Reilly and P.R.R. Langridge-Smith, *Organometallics*, **18**, 4090 (1999).
41. P.J. Dyson, *Adv. Organomet. Chem.*, **43**, 43 (1999).
42. H. Chen, Z. Tang, R. Huang and L. Zheng, *Eur. J. Mass Spectrom.*, **6**, 19 (2000).
43. P.J. Dyson, A.K. Hearley, B.F.G. Johnson, J.S. McIndoe and P.R.R. Langridge-Smith, *Inorg. Chem. Commun.*, **2**, 591 (1999).
44. W.J. Dollard, P.J. Dyson, T. Jackson, B.F.G. Johnson, J.S. McIndoe and P.R.R. Langridge-Smith, *Inorg. Chem. Commun.*, **2**, 587 (1999).
45. P.J. Dyson, J.E. McGrady, M. Reinhold, B.F.G. Johnson, J.S. McIndoe and P.R.R. Langridge-Smith, *J. Clust. Sci.*, **11**, 391 (2000).
46. P.J. Dyson, A.K. Hearley, B.F.G. Johnson, J.S. McIndoe and P.R.R. Langridge-Smith, *J. Chem. Soc., Dalton Trans.*, 2521 (2000).
47. A. Muller, E. Diemann, S. Qaiser Nazir Shah, C. Kuhlmann and M.C. Letzel, *Chem. Commun.*, 440 (2002).
48. S.W. Hunsucker, R.C. Watson, B.M. Tissue, *Rapid Commun. Mass Spectrom.*, **15**, 1334 (2001).
49. P.J. Dyson, A.K. Hearley, B.F.G. Johnson, J.S. McIndoe and P.R.R. Langridge-Smith, *J. Clust. Sci.*, **12**, 273 (2001).
50. P.J. Dyson, B.F.G. Johnson, J.S. McIndoe and P.R.R. Langridge-Smith, *Inorg. Chem.*, **39**, 2430 (2000).
51. P.J. Dyson, A.K. Hearley, B.F.G. Johnson, T. Khimyak, J.S. McIndoe and P.R.R. Langridge-Smith, *Organometallics*, **20**, 3970 (2001).
52. T.G. Schaaf, M.N. Shafigullin, J.T. Khoury, I. Vezmar and R.L. Whetten, *J. Phys. Chem. B*, **105**, 8785 (2001).
53. M.E. Barr, B.R. Adams, R.R. Weller and L.F. Dahl, *J. Am. Chem. Soc.*, **113**, 3052 (1991).
54. A. Bjarnason, R.E. Desenfants, M.E. Barr and L.F. Dahl, *Organometallics*, **9**, 657 (1990).
55. S. Martinovic, L.P. Tolic, D. Srzic, N. Kezele, D. Plavsic and L. Klasinc, *Rapid Commun. Mass Spectrom.*, **10**, 51 (1996).
56. N.C. Dopke, P.M. Treichel and M.M. Vestling, *Inorg. Chem.*, **37**, 1272 (1998).
57. R.W. McGaff, R.K. Hayashi, D.R. Powell and P.M. Treichel, *Polyhedron*, **17**, 4425 (1998).
58. C. Kim and I. Jung, *Inorg. Chem. Commun.*, **1**, 427 (1998).
59. C. Kim and I. Jung, *J. Organomet. Chem.*, **588**, 9 (1999).